International Journal of Heat and Mass Transfer 54 (2011) 4288–4299

Contents lists available at ScienceDirect

International Journal of Heat and Mass Transfer

journal homepage: www.elsevier.com/locate/ijhmt

Optimization of fluid flow and internal geometric structure of volumes cooled by forced convection in an array of parallel tubes

Paulo Canhoto *, A. Heitor Reis

Physics Department and Geophysics Centre of Évora, University of Évora, R. Romão Ramalho, 59, 7000-671 Évora, Portugal

ARTICLE INFO

Article history:
Received 31 December 2010
Received in revised form 13 May 2011
Available online 15 June 2011

Keywords:
Heat sinks
Forced convection
Laminar flow
Optimization
Intersection of asymptotes method

ABSTRACT

This paper reports the optimization of a heat sink composed of parallel tubes in a solid matrix of fixed dimensions for the following cases: (i) fixed pressure drop; (ii) fixed pumping power and (iii) fixed heat transfer rate density. The method of the intersection of asymptotes is employed using the dimensionless thermal length (x_*) as primary optimization variable, and approximate theoretical expressions for predicting the optimum ratio of diameter to tube length (D/L) are presented for each case. When the system is optimized with fixed heat transfer density it is found that the optimum values of both x_* and D/L are very close to those that correspond to the joint minimization of pressure drop and pumping power. These results are validated and complemented by means of numerical simulations.

1. Introduction

The design of forced convection heat sinks is usually carried out in order to maximize the heat transfer density under the maximum surface temperature allowed for the system to be cooled. In this case, the optimal internal geometric structure depends on the imposed constraint, e.g. fixed pressure drop or fixed pumping power. The same procedure is also used either for determining the maximum packaging of heat generating devices in a fixed volume or, conversely, if the heat generated is fixed and known, for minimizing the hot spot temperature. Two different approaches are commonly considered in heat sink optimization: (1) numerical simulations of flow and temperature fields and; (2) scale analysis of flow and heat transfer variables. Although the numerical simulation is more accurate, it requires computing time and resources that are not negligible as compared with the second approach. In the second approach, the method of the intersection of asymptotes [1,2] is a straightforward but powerful tool for predicting the optimal internal geometric structure of volumes cooled either by natural or forced convection, and is a tool of the constructal theory [3–5]. The constructal theory has extensive applicability in many domains, e.g. in optimization of engineered fluid flows and heat transfer networks [6,7], and prediction of shape and structure in natural systems [8,9] as well in living organisms [10]. The method of intersecting the asymptotes was first employed to predict the optimal spacing in a heat sink composed of parallel plates under natural convection [1], and thereafter applied to the optimization of a similar heat sink under forced convection and subjected to fixed pressure drop [2]. More recently, this last work was generalized to other duct geometries [11]. Optimization was also carried out for the case of a stack of heat generating boards with fixed mass flow rate and fixed pumping power [12] and for the cases of staggered plates [13] and cylinders in cross-flow [14,15]. Recent works report the use of the constructal method in the optimization of aspect ratios of channels with fixed pressure drop [16,17], and of metallic cellular sandwich heat sinks with constant pumping power [18]. The same method was used to design multi-scale compact micro-tube heat sinks [19] for maximum heat transfer density. Yilmaz et al. [20] carried out an asymptotic analysis of forced convection heat transfer in ducts of different shapes for laminar flow with fixed pressure drop, and used an exact method based on correlations to obtain the optimal geometry. More recently, the optimization of a heat sink composed of parallel circular or non-circular ducts in a finite volume was reported for the case of fixed pumping power constraint, see Ref. [21]. This work also reports the optimum length scale of ducts for pumping power minimization with fixed heat transfer density at a given nominal or maximum temperature of operation.

The method of intersecting the asymptotes provides the geometric point that optimizes the trade-off of two distinct trends. For example, in the case of a heat sink composed of parallel channels, for small hydraulic diameters the flow becomes fully developed and the outlet temperature of the fluid approaches the wall temperature, while for large hydraulic diameters the flow is thermally developing and the temperature of the fluid in the core

* Corresponding author. Tel.: +351 266740800; fax: +351 266745394.
E-mail addresses: canhoto@uevora.pt (P. Canhoto), ahr@uevora.pt (A.H. Reis).

0017-9310/$ - see front matter © 2011 Elsevier Ltd. All rights reserved.
doi:10.1016/j.ijheatmasstransfer.2011.05.016

Nomenclature

A	area (m^2)
c_p	specific heat ($J\,kg^{-1}\,K^{-1}$)
D	diameter (m)
D_h	hydraulic diameter (m)
f	friction factor
H	height (m)
h_{0-L}	average heat transfer coefficient ($W\,m^{-2}\,K^{-1}$)
L	length (m)
k	thermal conductivity ($W\,m^{-1}\,K^{-1}$)
$\dot{m}$	mass flow rate ($kg\,s^{-1}$)
N	number of tubes
p	pressure (Pa)
$\dot{P}_N$	total pumping power (W)
P_N^*	dimensionless pumping power, $\equiv \rho^2 L^4 \dot{P}_N/(\mu^3\, HWL)$
Pr	Prandtl number, $\equiv c_p\mu/k$
Nu_{0-L}	mean Nusselt number, $\equiv h_{0-L}D/k$
q''	heat flux ($W\,m^{-2}$)
$\dot{Q}_N$	total heat transfer rate (W)
Q_N^*	dimensionless heat transfer rate density, $\equiv L^2\,\dot{Q}_N/(k\,HWL(T_w - T_i))$
R	fluid flow resistance ($m^{-1}\,s^{-1}$)
r	radial coordinate (m)
Re	Reynolds number based on diameter, $\equiv U_0 D/\nu$
Re_L	Reynolds number based on length, $\equiv U_\infty L/\nu$
T	temperature (K)
U_0	mean fluid velocity in tubes (ms^{-1})
U_∞	free stream velocity (ms^{-1})
(u, v)	velocity components (ms^{-1})
x	axial coordinate (m)
x_+	dimensionless hydrodynamic length, $\equiv (L/D)/\mathrm{Re}$
x_*	dimensionless thermal length, $\equiv (L/D)/(\mathrm{Re\,Pr})$
W	width (m)

Greek symbols

α	thermal diffusivity ($m^2\,s^{-1}$), $\equiv k/(\rho c_p)$
Δp	pressure drop (Pa)
Δp^*	dimensionless pressure drop, $\equiv \rho L^2 \Delta p/\mu^2$
ε	volume fraction of tubes
μ	dynamic viscosity ($kg\,m^{-1}\,s^{-1}$)
ν	kinematic viscosity ($m^2\,s^{-1}$), $\equiv \mu/\rho$
ρ	density ($kg\,m^{-3}$)
θ	dimensionless temperature, $\equiv (T_w - T_o)/(T_w - T_i)$
τ_w	mean wall shear stress (Pa)

Subscripts

app	apparent
D_h	refers to hydraulic diameter
dv	developing
i	inlet
fd	fully developed
max	maximum
min	minimum
N	total for N tubes
o	outlet
opt	optimum
P_N	refers to fixed pumping power
Q_N	refers to fixed heat transfer density
w	wall
Δp	refers to fixed pressure drop

Superscript

$(\tilde{})$	dimensionless variables, Eqs. (23)–(26)

remains nearly unchanged. It is also possible to represent these limiting cases in terms of the dimensionless thermal length of the flow (x_*), thus allowing to directly verify if the fluid is 'efficiently used' for the cooling purpose: (i) if x_* is too small it means that the fluid in the core flow almost do not participate in the heat transfer process and; (ii) if x_* is too large the heat flux decreases and, in the limit, no more heat can be extracted by the fluid. The intersection of these two distinct trends makes it possible to predict the optimum length scale of the heat sink channels together with the optimum dimensionless thermal length under global constraints. For example, for a parallel plates heat sink subjected to fixed pressure drop the intersection of asymptotes underestimates by only 12% the optimum plate-to-plate spacing for maximum heat transfer density [2]. In this case the adjacent thermal boundary layers merge just at the exit of the channel. However, we can recognize the concept beyond this method as a general rule that is likely independent of the imposed fluid flow constraints, because thermally developed and developing flow limits are still possible to reach if diverse conditions are considered. Specifically, we may assume that the method is able not only to predict the optimal internal geometric structure but also provide some guidelines about the better fluid flow conditions for a given heat transfer density. The fluid flow constraint depends on the flow arrangement in which the heat sink is connected [12]. If several heat sinks or other components are connected in parallel thus receiving the flow from the same plenum then the fixed pressure drop is the appropriate constraint, while fixed mass flow rate constraint reveals appropriate when several components are placed in series. If a heat sink is the only component that is cooled by the flow imposed by a pump or fan, then the fixed pumping power assumption must be used. However, in this case we must also consider pumping power minimization with fixed heat transfer density, because in several practical installations the heat to be extracted from a system or device at a given design or maximum temperature is known, and the objective is reducing the electric power input to the fan or pump.

In this work, we explore the concept of the method of intersecting the asymptotes for the optimization of a heat sink composed of parallel tubes, by considering different constraints: fixed pressure drop, fixed pumping power, and fixed heat transfer density. The dimensionless thermal length is used as the primary optimization variable and the optimum ratio of diameter to tube length (D/L) is obtained for each case together with the maximum heat transfer density, minimum pressure drop or minimum pumping power. These results are validated and complemented by numerical simulations of fluid flow and temperature fields.

2. Hydrodynamic and thermal analysis of heat sink optimization

The heat sink under consideration in the present work is composed of parallel tubes in a solid matrix of high thermal conductivity material with fixed dimensions H, W and L, as shown in Fig. 1(a). The number of tubes with diameter D in the array is given by

$$N \simeq \frac{4\varepsilon HW}{\pi D^2}. \tag{1}$$

The volume fraction of the tubes ε is set fixed by the heat sink designer. For example, in the case of circular tubes in a maximum packing square arrangement $\varepsilon \simeq 0.785$ and $N \simeq HW/D^2$. A coolant

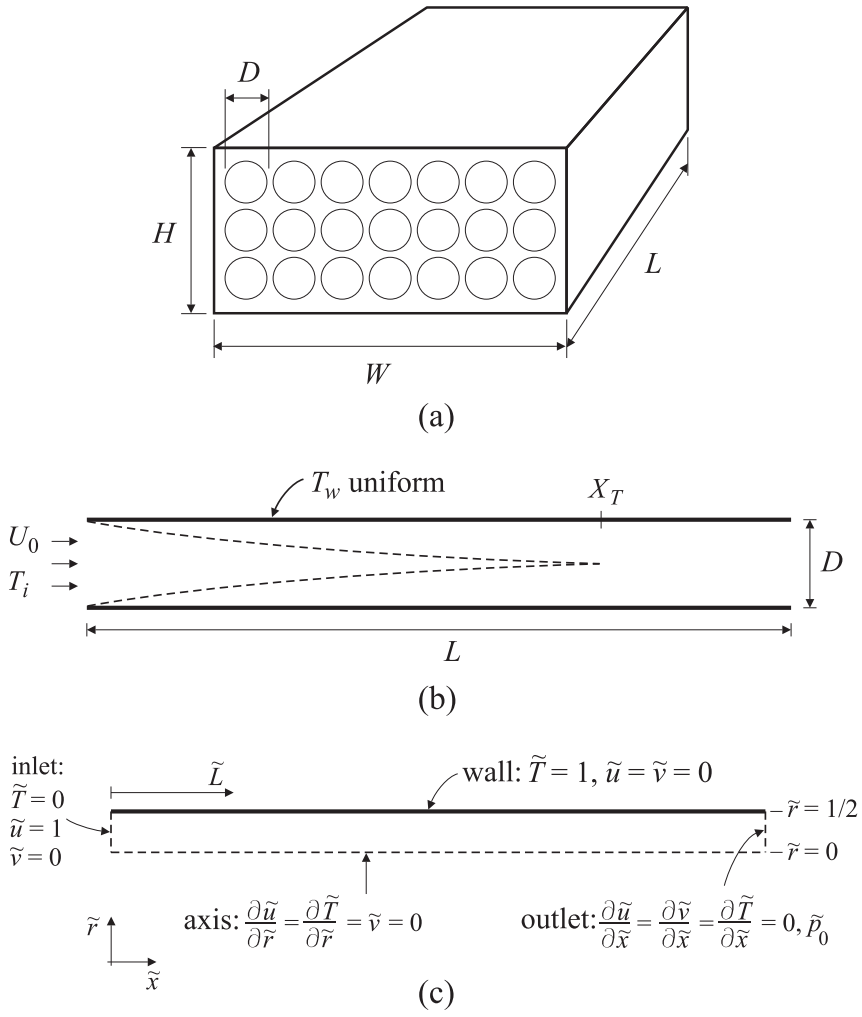

Fig. 1. Compact heat sink of parallel ducts in a finite volume: (a) geometry schematic; (b) physical domain of an elemental channel; (c) computational domain and boundary conditions.

flows in the tubes with mean velocity U_0 and inlet temperature T_i. It is assumed that the flow is steady, laminar, incompressible, and equally distributed among the tubes, together with negligible pressure losses at the inlet and outlet plenums. The walls of the tubes are considered to be at uniform temperature T_w, thus neglecting the conduction resistance in the solid matrix, in line with recent works for similar multilayer channel configuration [11,17–21]. This also means that we can regard T_w as the scale of the surface temperature, which is distinct from the inlet and outlet temperatures of the fluid. Additionally, it is assumed that the thermodynamic and transport properties of the fluid are constant.

The mass flow rate in each tube is given by:

$$\dot{m} = \rho U_0 \pi D^2/4, \tag{2}$$

while the total rate of heat removed from the heat sink reads:

$$\dot{Q}_N = N\dot{m}c_p(T_o - T_i). \tag{3}$$

The mean temperature of the fluid at the outlet T_o is determined through the following expression [22]:

$$\theta = \frac{T_w - T_o}{T_w - T_i} = \exp\left(-4x_*\mathrm{Nu}_{0-L}\right), \tag{4}$$

where Nu_{0-L} is the mean Nusselt number and x_* is the dimensionless thermal length, which reads:

$$x_* = \frac{L/D}{\mathrm{Re}\,\mathrm{Pr}}. \tag{5}$$

By combining Eqs. (1)–(4) one finds the total heat transfer rate in the form:

$$\dot{Q}_N = \varepsilon HW\frac{\rho k}{\mu}\mathrm{Pr}U_0(1-\theta)(T_w - T_i). \tag{6}$$

The mean fluid velocity U_0 is related to the pressure drop across the heat sink through the apparent friction factor method by using the known formula:

$$\frac{\Delta p}{1/2\rho U_0^2} = 4x_+ f_{\mathrm{app}}\,\mathrm{Re} \tag{7}$$

with the friction factor-Reynolds number group given by [23]

$$f_{\mathrm{app}}\,\mathrm{Re} = \left[\left(\frac{3.44}{x_+^{1/2}}\right)^2 + (f\,\mathrm{Re})^2\right]^{1/2}. \tag{8}$$

Note that the dimensionless hydrodynamic length $x_+ = (L/D)/\mathrm{Re}$ may also read $x_+ = x_*\,\mathrm{Pr}$ and that f Re stands for friction factor of fully developed flow. More recently, Muzychka and Yovanovich [24,25] presented a detailed analysis of heat transfer and friction

factor in circular and non-circular ducts and proposed new models for developing and fully developed flow. By combining Eqs. (6) and (7) we obtain

$$\dot{Q}_N = \underbrace{(\varepsilon H\ W)}_{\text{Geometry}}\ \underbrace{(\rho^{1/2}\mathrm{Pr}^{1/2}k/\mu)}_{\text{Fluid properties}}\ \underbrace{(2x_*f_{app}\mathrm{Re})^{-1/2}}_{\text{Fluid flow}} \times \underbrace{(1-\theta)}_{\text{Heat transfer}}\ \Delta p^{1/2}(T_w - T_i) \tag{9}$$

In the right hand side of this equation four groups of factors are identified that relate to overall geometry, fluid properties and fluid flow and heat transfer conditions, respectively. Considering that both f_{app} Re and Nu_{0-L} can be determined as functions of dimensionless thermal length and Prandtl number, then x_* emerges as the unique free variable in Eq. (9) that can be adjusted for maximum heat transfer rate.

From previous works on heat sink optimization [2,11,20] it is known that when the imposed pressure drop is fixed an optimal internal geometry exists for which the total heat transfer rate is maximum. In fact, as for a given Pr both f Re and Nu_{0-L} decrease with x_*, and by a simple graphical analysis of Eq. (9) (not shown here for concision, see the next sections), if both Δp and $(T_w - T_i)$ are fixed we conclude that a maximum value of $\dot{Q}_N$ exists for a certain value of x_* (optimum). What is important to retain now is that the group $(1-\theta)x_*^{-1/2}$ makes it possible this maximum to exist, also for thermally developing flow (f Re = 16). If we rewrite Eq. (9) in the following simplified form:

$$\frac{\dot{Q}_N}{\Delta p^{1/2}(T_w - T_i)} = f(x_*), \tag{10}$$

where $f(x_*) > 0$ stands for the four groups of factors identified before, it is straightforward to show that the optimum value of x_* that emerges from $\partial f(x_*)/\partial x_* = 0$ may be found either through maximization of $\dot{Q}_N$ at constant Δp and $T_w - T_i$, or equivalently through minimization of either Δp (at constant $\dot{Q}_N$ and $T_w - T_i$) or $T_w - T_i$ (at constant $\dot{Q}_N$ and Δp). The relation between D/L, x_* and Δp may be derived from Eqs. (5) and (7) with $U_0 = \nu\ \mathrm{Re}/D$:

$$D/L = \left(\frac{2f_{app}\mathrm{Re}}{x_*\mathrm{Pr}}\right)^{1/4} \Delta p^{*-1/4}, \tag{11}$$

where $\Delta p^* = \rho L^2 \Delta p/\mu^2$ is dimensionless pressure drop. Once the optimum x_* is known, the optimum ratio of diameter to tube length can be determined through Eq. (11) by using either the fixed value or the minimum value of pressure drop. In the case of heat transfer rate maximization the value of $(\dot{Q}_N)_{\max}$ is determined by making $x_* = (x_*)_{\text{opt}}$ in Eq. (9), which can be rewritten in the following form:

$$Q_N^*/\varepsilon = (2x_*f_{app}\mathrm{Re})^{-1/2}\ (1-\theta)\ \mathrm{Pr}^{1/2}\Delta p^{*1/2}, \tag{12}$$

with

$$Q_N^* = \frac{L^2\dot{Q}_N/(HWL)}{k(T_w - T_i)}, \tag{13}$$

which is dimensionless heat transfer density. From this analysis we may conclude that both the optimum dimensionless thermal length and the optimum D/L ratio are independent of porosity ε while the maximum heat transfer rate density varies with ε at fixed Δp, and the minimum pressure drop varies with ε^{-2} at fixed $\dot{Q}_N$. Furthermore, one can verify that the maximum heat transfer rate scales with the group $(\mathrm{Pr}\ \Delta p^*)^{1/2}$ while the optimum diameter scales with $(\mathrm{Pr}\ \Delta p^*)^{-1/4}$.

If the mean velocity U_0 is related to the total pumping power in the form

$$\dot{P}_N = \frac{1}{\rho} N \dot{m} \Delta p, \tag{14}$$

then, by using Eqs. (1), (2), (6), and (7), the heat transfer rate reads:

$$\dot{Q}_N = \underbrace{(\varepsilon HW)^{2/3}}_{\text{Geometry}}\ \underbrace{(\rho^{2/3}\mathrm{Pr}^{2/3}k/\mu)}_{\text{Fluid properties}}\ \underbrace{(2x_*f_{app}\mathrm{Re})^{-1/3}}_{\text{Fluid flow}} \times \underbrace{(1-\theta)}_{\text{Heat transfer}}\ \dot{P}_N^{1/3}(T_w - T_i). \tag{15}$$

Again, the dimensionless thermal length is the unique optimization variable. Similarly to the case before, by rewriting the last equation in the form:

$$\frac{\dot{Q}_N}{\dot{P}_N^{1/3}(T_w - T_i)} = g(x_*), \tag{16}$$

where $g(x_*) > 0$ stands for the four groups of factors identified in the right-hand side of Eq. (15), we can easily verify that the optimum value of x_* that emerges from $\partial g(x_*)/\partial x_* = 0$ may be found either when maximizing $\dot{Q}_N$ at constant $\dot{P}_N$ and $T_w - T_i$, or either when minimizing $\dot{P}_N$ (at constant $\dot{Q}_N$ and $T_w - T_i$) or $T_w - T_i$ (at constant $\dot{Q}_N$ and $\dot{P}_N$). Here, the existing extreme comes from the group $(1-\theta)x_*^{-1/3}$. The relation between D/L, x_* and $\dot{P}_N$ is obtained from Eqs. (1), (2), (5), (7), and (14) with $U_0 = \nu\ \mathrm{Re}/D$:

$$D/L = \left(\frac{(2f_{app}\mathrm{Re})^{1/2}}{x_*\mathrm{Pr}}\right)^{1/3} (P_N^*/\varepsilon)^{-1/6}, \tag{17}$$

where $P_N^* = \rho^2 L^4 \dot{P}_N/(\mu^3 HWL)$ is dimensionless pumping power. Again, once the optimum x_* is known the optimum ratio of diameter to tube length can be determined through Eq. (17) by using either the fixed value or the minimum value of pumping power. In the case of heat transfer rate maximization the value of $(\dot{Q}_N)_{\max}$ is determined by making $x_* = (x_*)_{\text{opt}}$ in Eq. (15), which can be rewritten in the following dimensionless form

$$Q_N^*/\varepsilon = (2x_*f_{app}\mathrm{Re})^{-1/3}\ (1-\theta)\ \mathrm{Pr}^{2/3}(P_N^*/\varepsilon)^{1/3}. \tag{18}$$

Note that the groups Q_N^*/ε and P_N^*/ε represent the dimensionless heat transfer rate and total pumping power per unit of volume that is effectively occupied by the fluid, respectively. In this case we may conclude that the optimum dimensionless thermal length is independent of ε while the optimum D/L ratio varies with $\varepsilon^{1/6}$, the maximum heat transfer rate density varies with $\varepsilon^{2/3}$ at fixed $\dot{P}_N$, and the minimum pumping power varies with ε^{-2} at fixed $\dot{Q}_N$. One can also verify that the maximum Q_N^*/ε scales with the group $\mathrm{Pr}^{2/3}(P_N^*/\varepsilon)^{1/3}$ while the optimum diameter scales with $\mathrm{Pr}^{-1/3}(P_N^*/\varepsilon)^{-1/6}$.

3. Numerical heat sink modelling

The physical domain of one single tube of the heat sink together with the computational domain and the boundary conditions are shown in Fig. 1. The dimensionless governing equations for steady flow in cylindrical coordinates read:

Continuity

$$\frac{\partial \tilde{u}}{\partial \tilde{x}} + \frac{\tilde{v}}{\tilde{r}} + \frac{\partial \tilde{v}}{\partial \tilde{r}} = 0, \tag{19}$$

x-momentum

$$\tilde{u}\frac{\partial \tilde{u}}{\partial \tilde{x}} + \tilde{v}\frac{\partial \tilde{u}}{\partial \tilde{r}} = -\frac{\partial \tilde{p}}{\partial \tilde{x}} + \frac{1}{\mathrm{Re}}\left(\frac{\partial^2 \tilde{u}}{\partial \tilde{x}^2} + \frac{1}{\tilde{r}}\frac{\partial \tilde{u}}{\partial \tilde{r}} + \frac{\partial^2 \tilde{u}}{\partial \tilde{r}^2}\right), \tag{20}$$

r-momentum

$$\tilde{u}\frac{\partial \tilde{v}}{\partial \tilde{x}} + \tilde{v}\frac{\partial \tilde{v}}{\partial \tilde{r}} = -\frac{\partial \tilde{p}}{\partial \tilde{r}} + \frac{1}{\mathrm{Re}}\left(\frac{\partial^2 \tilde{v}}{\partial \tilde{x}^2} - \frac{\tilde{v}}{\tilde{r}^2} + \frac{1}{\tilde{r}}\frac{\partial \tilde{v}}{\partial \tilde{r}} + \frac{\partial^2 \tilde{v}}{\partial \tilde{r}^2}\right). \tag{21}$$

Energy

$$\tilde{u}\frac{\partial\tilde{T}}{\partial\tilde{x}}+\tilde{v}\frac{\partial\tilde{T}}{\partial\tilde{r}}=\frac{1}{\mathrm{RePr}}\left(\frac{\partial^2\tilde{T}}{\partial\tilde{x}^2}+\frac{1}{\tilde{r}}\frac{\partial\tilde{T}}{\partial\tilde{r}}+\frac{\partial^2\tilde{T}}{\partial\tilde{r}^2}\right). \quad (22)$$

The axial and radial velocity components are $\tilde{u}$ and $\tilde{v}$, respectively. These equations are obtained by defining the following variables transformations

$$(\tilde{u},\tilde{v})=(u,v)/U_0, \quad (23)$$

$$(\tilde{x},\tilde{r},\tilde{L})=(x,r,L)/D, \quad (24)$$

$$\tilde{p}=p/(\rho U_0^2), \quad (25)$$

$$\tilde{T}=\frac{T-T_i}{T_w-T_i}. \quad (26)$$

No-slip condition at the wall and zero gradients at the outlet boundary are assumed. The heat transfer rate is calculated from the local heat flux at the wall $q'=k(\partial T/\partial r)_{r=D/2}$. The governing equations were solved with the help of the finite volume method by using a free source code for convection–diffusion problems [26]. The diffusion terms were discretised by means of a central differencing scheme, and convergence was considered to be achieved when the normalized residuals of the mass and momentum equations became smaller than 10^{-6}, and the residual of the energy equation smaller than 10^{-8}. A grid independence test was carried out for the following conditions: $D=0.004$ m, $L=0.10$ m, $U_0=0.1$ m/s and $\mathrm{Pr}=5.0$. The numerical values generated in this simulation test were validated by comparison with the results presented in referenced literature [27], and it was found that mesh size of 100×50 assures a grid independent solution.

From the analysis presented in the previous section we concluded that the same value of optimum x_* is obtained either when maximizing heat transfer density or when minimizing either pressure drop or pumping power at fixed heat transfer density. Furthermore, the optimum x_* is independent of the volume fraction of tubes. Thus, the numerical simulations were carried out considering the following fixed values: $Q_N^*=1\times10^3$, $\varepsilon=0.6$ and $V=1\times10^{-4}$ m^3.

In the case of simultaneously developing flow the numerical procedure can be briefly described as comprising the following steps: (1) obtain the fluid flow and temperature fields in a long tube ($D/L\leqslant0.01$) for a given Reynolds number; (2) assume an initial number of tubes; (3) find the D/L ratio to obtain the required heat transfer density; (4) update the number of tubes and the D/L ratio according to the fixed volume constraint; (5) calculate the dimensionless thermal length, the pressure drop and the pumping power. The procedure above is repeated for various Reynolds numbers within the laminar fluid flow range and such that the dimensionless thermal length falls in the range $10^{-4}<x_*<0.5$. The minimum pressure drop and the minimum pumping power are obtained with the help of an external numerical minimization procedure.

In the particular case of hydrodynamically fully developed flow the radial velocity component is zero and the axial component is $\tilde{u}=2(1-4\tilde{r}^2)$. Then, by neglecting the effect of axial conduction ($\mathrm{Re\,Pr}\gg1$), the energy conservation equation reduces to the classical Graetz problem formulation [28]. In this case the heat transfer rate is well modelled by using an appropriate estimate for the mean Nusselt number in Eqs. (12) and (18) along with $f\,\mathrm{Re}=16$. We modelled the Nusselt number of thermally developing flow as:

$$\mathrm{Nu}_{dv}=1.522x_*^{-1/3}. \quad (27)$$

This equation is deduced during the scale analysis presented in the next section and is very similar to the Lévêque solution ($\mathrm{Nu}_{dv}=1.615x_*^{-1/3}$) [29]. Then, the asymptotic correlation method outlined by Churchill and Usagi [30] was used to model the Nusselt number in the entire range of x_* in the form:

$$\mathrm{Nu}_{0-L}=\left(\mathrm{Nu}_{dv}^4+\mathrm{Nu}_{fd}^4\right)^{1/4} \quad (28)$$

with $\mathrm{Nu}_{fd}=3.66$. The values generated by Eq. (28) were compared with data from Shah and London [31] and maximum differences were found within −0.96% to 0.62% for $x_*\geqslant1\times10^{-3}$. These differences fall in the range −3.04% to 0.62% for $x_*\geqslant1\times10^{-4}$.

4. Scale analysis and intersection-of-asymptotes method

In the first part of this section, we present scale analysis and the method of intersection of asymptotes for predicting the optimal heat sink design that maximizes the heat transfer density with fixed pressure drop and fixed pumping power. In the second part, we present scale analysis of fluid flow optimization (minimization of pressure drop and pumping power) with fixed heat transfer density.

4.1. Scale analysis of heat transfer rate maximization

Bejan and Sciubba [2] and more recently Muzychka [11] used the method of the intersection of asymptotes for optimizing a parallel channels heat sink subjected to finite volume and fixed pressure drop constraints. In those works the optimal internal structure was predicted for maximum heat transfer rate, with the optimization variable D either representing the plate-to-plate spacing or the inner circular tube diameter or else other reference length scale of the duct shape. In that case, the mean velocity of the fluid (or equivalently the Reynolds number) and the dimensionless thermal length x_* implicitly vary according to the flow constraint. The method is based on the intersection of two distinct trends: (i) the fully developed flow asymptote ($D\to0$ limit), in which the mean outlet temperature of the fluid approaches the temperature of the wall and the heat transfer rate varies as $\sim D^2$; and (ii) the developing flow asymptote ($D\to\infty$ limit), in which the mean temperature of the fluid in the flow core approaches the inlet temperature, and the total heat transfer rate varies as $\sim D^{-2/3}$. In this section, the method of the intersection of asymptotes is employed using x_* as the optimization variable and for the cases when either pressure drop or pumping power are fixed. Firstly, the method is applied for the case of thermally developing flow and then the results are generalized for simultaneously developing flow, and formulae for predicting the optimum diameter of the tubes are presented.

4.1.1. Fixed pressure drop

In the fully developed flow limit the total heat transfer rate is given by the global energy balance in the array:

$$\dot{Q}_{fd}=N\dot{m}c_p(T_w-T_i). \quad (29)$$

The mass flow rate $\dot{m}$ or, alternatively, the mean velocity of the fluid in the tubes U_0 is related to pressure drop Δp through Eq. (7), where the friction factor-Reynolds number group in the case of circular tubes and fully hydrodynamically developed flow is $f\,\mathrm{Re}=16$. Then, by setting $x_*=x_+/\mathrm{Pr}$ as the optimization variable, the mean velocity reads:

$$U_0=\left(\frac{\Delta p}{2f\mathrm{Re}\rho\mathrm{Pr}x_*}\right)^{1/2}. \quad (30)$$

By combining Eqs. (1), (2), (29), and (30), and with Prandtl number given by $\mathrm{Pr} = \mu c_p/k$, the total rate of heat transfer reads:

$$\dot{Q}_{fd} = \varepsilon HW\left(\frac{\rho \mathrm{Pr}\Delta p}{2f\mathrm{Re}\mu^2 x_*}\right)^{1/2} k(T_w - T_i). \tag{31}$$

This expression can be rewritten in dimensionless form as (see Eq. (13)):

$$Q^*_{fd} = \varepsilon\left(\frac{\mathrm{Pr}\Delta p^*}{2f\mathrm{Re}}\right)^{1/2} x_*^{-1/2} \tag{32}$$

Thus, in the limit $x_* \to \infty$ the heat transfer density varies as $x_*^{-1/2}$. The group $Be = \mathrm{Pr}\,\Delta p^*$ that appears in the last equation is also referred as the Bejan number [32].

In the thermally developing flow limit the total heat transfer rate that is removed from the entire array of tubes with transfer area $A_N = N\pi DL$ is given by

$$\dot{Q}_{dv} = A_N h_{0-L}(T_w - T_i). \tag{33}$$

The average heat transfer coefficient h_{0-L} may be approximated by the expression for laminar boundary layer flow over a flat plate [11,28]:

$$\frac{Lh_{0-L}}{k} = 0.664\mathrm{Re}_L^{1/2}\mathrm{Pr}^{1/3} \tag{34}$$

for $\mathrm{Pr} \geqslant 0.5$. The Reynolds number based on the length Re_L is obtained from balancing the forces on the array:

$$\tau_w N\pi DL = N\frac{\pi D^2}{4}\Delta p \tag{35}$$

in which the mean wall shear stress τ_w is given by the velocity boundary layer solution [28]

$$\frac{\tau_w}{1/2\rho U_\infty^2} = 1.328\,\mathrm{Re}_L^{-1/2} \tag{36}$$

and U_∞ is the free stream (core flow) velocity. Combining Eqs. (35) and (36) with $U_\infty = \nu\,\mathrm{Re}_L/L$ yields:

$$\mathrm{Re}_L^{1/2} = 0.722\,\Delta p^{*1/3}\,(D/L)^{1/3}. \tag{37}$$

The use of the square root of Re_L instead of the free stream velocity U_∞ is advantageous because $\mathrm{Re}_L^{1/2}$ accounts for the boundary layer slenderness ratio as noted by Bejan [28]. Finally, by combining Eqs. (11), (33), (34), and (37) we obtain the dimensionless heat transfer density in the form:

$$Q^*_{dv} = 1.918\,\varepsilon\frac{(\mathrm{Pr}\Delta p^*)^{1/2}}{(2f\mathrm{Re})^{1/6}}x_*^{1/6}. \tag{38}$$

Eq. (38) shows that in the limit $x_* \to 0$ the global heat transfer density varies as $\sim x^{1/6}$.

It is worth noting that by combining Eqs. 34 and 37 and eliminating the pressure drop through Eq. (11) we obtain the mean Nusselt number based on D in the form:

$$\frac{Dh_{0-L}}{k} = 0.604(f\mathrm{Re})^{1/3}x_*^{-1/3}, \tag{39}$$

which in the case of circular tubes ($f\,\mathrm{Re} = 16$) reduces to

$$\frac{Dh_{0-L}}{k} = 1.522x_*^{-1/3}. \tag{40}$$

This expression was already presented in the previous section (see Eq. (27)) (the difference to data [31] is smaller than 3.04% in the range $1\times10^{-4} \leqslant x_* \leqslant 1\times10^{-2}$). Eq. (39) still holds for other duct geometries provided that the correspondent hydraulic diameter and friction factor-Reynolds number group are used, and good agreement can also be found for square and parallel plate channels. This confirms the correctness of the approximations assumed in the formulation of the developing flow asymptote and corresponds to $(\tau_w)_{plate} = (\tau_w)_{tube}$, i.e., the average heat transfer coefficient of a thermally developing flow in a circular tube is quite well described by the boundary layer solution of Eq. (34) when using values of $\mathrm{Re}_L^{1/2}$ such that the mean gradient of the fluid velocity near a flat plate surface $\overline{(\partial u/\partial y)}_{y=0}$ (that is the fluid that effectively participates in the heat transfer) is equal to the gradient of the fluid velocity at the wall of the tube.

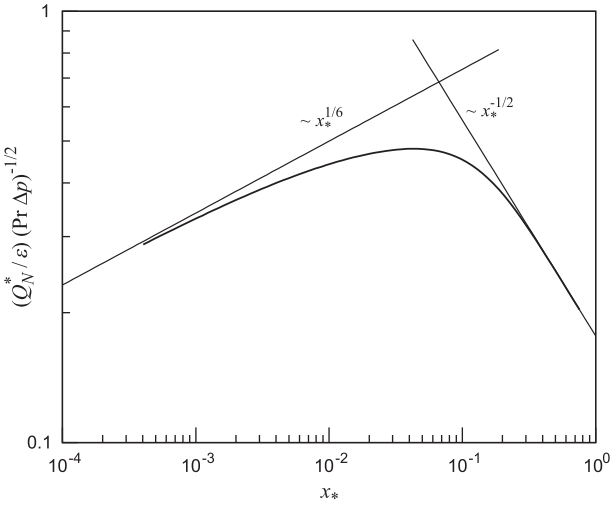

Fig. 2. Heat transfer asymptotes as function of dimensionless thermal length at fixed pressure drop.

The asymptotes described by Eqs. (32) and (38) as well as the actual dimensionless heat transfer density from Eq. (12) are depicted in Fig. 2. The optimum x_* that emerges from the intersection of these asymptotes is given by

$$(x_*)_{\mathrm{opt}} = \frac{1}{1.918^{3/2}(2f\mathrm{Re})^{1/2}}, \tag{41}$$

while the optimum ratio of diameter to tube length can be predicted through Eq. (11) by making $x_* = (x_*)_{\mathrm{opt}}$:

$$(D_h/L)_{\mathrm{opt}} \approx 1.277(2f\mathrm{Re}_{D_h})^{3/8}(\mathrm{Pr}\Delta p^*)^{-1/4}. \tag{42}$$

This equation is intentionally presented in its generalized form based on hydraulic diameter with the purpose of highlighting two aspects: (i) the present result still holds for other duct geometries, in particular, we note that the application of Eq. (42) to parallel plates heat sink ($D_h = 2D$, $f\mathrm{Re}_{D_h} = 24$) leads to $D_{opt}/L \cong 2.73Be^{-1/4}$ with $Be = \mathrm{Pr}\,\Delta p^*$, which matches exactly the optimum plate-to-plate spacing (D_{opt}) found by Bejan [2] for that geometry; and (ii) Eq. (42) is a straightforward form alternative to the result obtained by Muzychka [11] that used the geometric length scale D_h as optimization variable in the case of simultaneously developing flow.

In the case of the present work, for circular tubes we have $(x_*)_{\mathrm{opt}} \approx 0.067$ and

$$D_{\mathrm{opt}}/L \approx 4.684(\mathrm{Pr}\Delta p^*)^{-1/4} \tag{43}$$

As conclusion, we can extend the use of Eqs. (42) and (43) to simultaneously developing flow and, by comparison with Eq. (11), to find out $(x_*)_{\mathrm{opt}}$ from

$$\left(\frac{2f_{app}\mathrm{Re}}{(x_*)_{\mathrm{opt}}}\right)^{1/4} = 4.684 \tag{44}$$

The solution of this equation depends on Prandtl number due to the relation between dimensionless hydrodynamic and thermal lengths $x_+ = x_* \mathrm{Pr}$. A polynomial equation on $(x_*)_{opt}$ is obtained by substituting Eq. (8) in Eq. (44), and the optimum x_* decreases and approaches 0.067 for $\mathrm{Pr} \gg 1$. The feasible solution of this polynomial equation is presented and discussed in Section 5 for various values of Pr.

From Eq. (32) (or Eq. (38)) one finds that the maximum heat transfer density corresponding to $x_* = (x_*)_{opt}$ is given by:

$$(Q_N^*/\varepsilon)_{max} < 1.630\,(2f\mathrm{Re})^{-1/4}(\mathrm{Pr}\Delta p^*)^{1/2}. \tag{45}$$

The maximum heat transfer density is directly proportional to ε and to the square root of Prandtl number. In the case of a parallel tubes heat sink in a maximum square packing arrangement ($\varepsilon \approx 0.785$) one has $Q^*_{N,max} < 0.538(\mathrm{Pr}\Delta p^*)^{1/2}$.

4.1.2. Fixed pumping power

The heat transfer asymptotes at fixed pumping power can be derived in a way similar to that of fixed pressure drop. Again, we start by considering a thermally developing flow. By using Eqs. (7) and (14) together with Eqs. (1) and (2) the mean velocity reads:

$$U_0 = \left(\frac{\dot{P}_N}{\varepsilon HW 2f\mathrm{Re}\,\rho \mathrm{Pr} x_*}\right)^{1/3}, \tag{46}$$

while pressure drop relates to pumping power as:

$$\Delta p^* = (2f\mathrm{Re}x_*\mathrm{Pr})^{1/3}\left(\frac{P_N^*}{\varepsilon}\right)^{2/3} \tag{47}$$

Then, by using Eqs. (32) and (47) the fully developed flow asymptote reads:

$$Q^*_{fd} = \frac{\varepsilon^{2/3}}{(2f\mathrm{Re})^{1/3}}\mathrm{Pr}^{2/3}P_N^{*1/3}x_*^{-1/3}. \tag{48}$$

Thus, in the limit $x_* \to \infty$ the heat transfer density varies with $x_*^{-1/3}$. In the same way the developing flow asymptote of Eq. (38) turns into:

$$Q^*_{dv} = 1.918\varepsilon^{2/3}\mathrm{Pr}^{2/3}P_N^{*1/3}x_*^{1/3}, \tag{49}$$

In the limit $x_* \to 0$ the heat transfer density varies with $x_*^{1/3}$. It must be also noted that this asymptote is independent of the duct shape. Both the asymptotes and the actual dimensionless heat transfer density calculated from Eq. (18) are shown in Fig. 3. Due to proportionality between pressure drop and pumping power shown by Eq. (47), it is expected that the intersection of the asymptotes with fixed P_N^* will predict the same optimum x_* as with the asymptotes at fixed Δp^*. In fact, from the combination of Eqs. (48) and (49) we obtain again Eq. (41). This shows that in the case of thermally developing flow, the optimum x_* predicted by intersecting the asymptotes is independent of the constraint imposed to fluid flow.

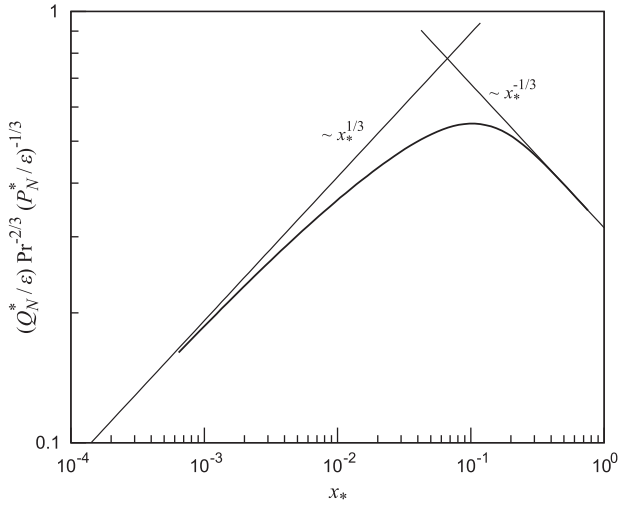

Fig. 3. Heat transfer asymptotes as function of dimensionless thermal length at fixed pumping power.

The optimum ratio of diameter to tube length is predicted by making $x_* = (x_*)_{opt}$ in Eq. (17):

$$(D_h/L)_{opt} \approx 1.385\,(2f\mathrm{Re}_{D_h})^{1/3}\mathrm{Pr}^{-1/3}(P_N^*/\varepsilon)^{-1/6}. \tag{50}$$

Again we present a generalization based on the hydraulic diameter to show that this result still holds for other duct geometries. In particular, we note that the application of Eq. (50) to a parallel plates heat sink ($D_h = 2D$, $f\mathrm{Re}_{D_h} = 24$, $\varepsilon = 1$) yields $D_{opt}/L \cong 2.52\mathrm{Pr}^{-1/3}P_N^{*-1/6}$, which is similar and matches the optimum plate-to-plate spacing (D_{opt}) found by Mereu et al. [12] very closely, in which the dimensionless pumping power raised to the power $-1/6$ is multiplied by the group $2.26\,\mathrm{Pr}^{-10/27}$. The result by Mereu was obtained by using the plate-to-plate spacing as the optimization (free) variable together with simultaneously developing flow, and assuming that the mean velocity of the fluid U_0 is equal to the free stream velocity U_∞ when deriving the developing flow asymptote. The values of $(D_h/L)_{opt}$ obtained from the present work are tabulated and summarized in Table 1 for some duct geometries. In the case of circular tubes we have $(x_*) \approx 0.067$ and

$$D_{opt}/L \approx 4.397\mathrm{Pr}^{-1/3}(P_N^*/\varepsilon)^{-1/6}. \tag{51}$$

We can extend the use of Eqs. (50) and (51) to simultaneously developing flow and, by comparison with Eq. (17), determine $(x_*)_{opt}$ for that case from:

$$\left(\frac{(2f_{app}\mathrm{Re})^{1/2}}{(x_*)_{opt}}\right)^{1/3} = 4.397. \tag{52}$$

The optimum x_* decreases and approaches 0.067 for $\mathrm{Pr} \gg 1$, and the results for various values of Prandtl number are presented in Section 5.

The maximum heat transfer density is predicted through Eq. (48) (or Eq. (49)) and is given by:

$$(Q_N^*/\varepsilon)_{max} < 1.385\,(2f\mathrm{Re}_{D_h})^{-1/6}\mathrm{Pr}^{2/3}(P_N^*/\varepsilon)^{1/3}. \tag{53}$$

The maximum heat transfer density is proportional to $\varepsilon^{2/3}$ and varies with $\mathrm{Pr}^{2/3}$. The estimated values of maximum Q_N^* are presented in Table 1 for some duct geometries. In the case of a parallel tubes heat sink with $\varepsilon \approx 0.785$ we have $Q^*_{N,max} < 0.661\,\mathrm{Pr}^{2/3}P_N^{*1/3}$.

4.2. Scale analysis of fluid flow optimization with fixed heat transfer density

In this section we present a scale analysis of fluid flow optimization with fixed heat transfer density through the method of the intersection of asymptotes, allowing predicting the optimum D/L

Table 1
Values of optimum hydraulic diameter $(D_h/L)_{opt}\mathrm{Pr}^{1/3}(P_N^*/\varepsilon)^{1/6}$ and maximum heat transfer density $(Q_N^*/\varepsilon)_{max}\mathrm{Pr}^{-2/3}(P_N^*/\varepsilon)^{-1/3}$ as predicted by the method of the intersection of asymptotes for different duct geometries at fixed pumping power.

Duct geometry	D_h	$f\mathrm{Re}_{D_h}$	Optimum D_h	Maximum Q_N^*
Parallel plates	$2D$	24	5.033	0.727
Circular tube	D	16	4.397	0.777
Square	D	14.24	4.230	0.793
Equilateral triangle	$D/\sqrt{3}$	13.33	4.137	0.801

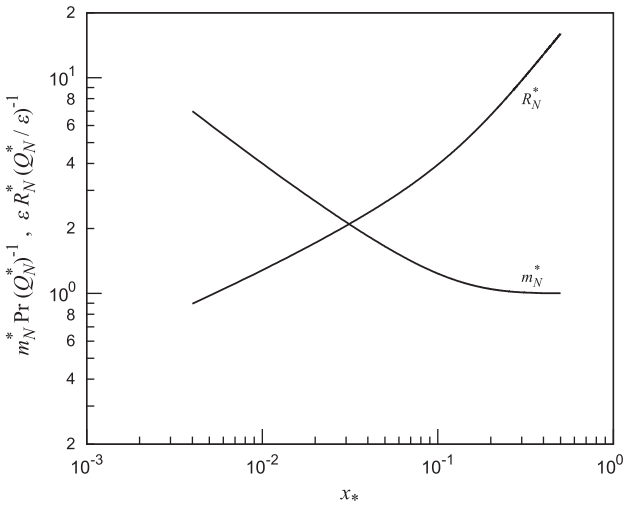

Fig. 4. Dimensionless mass flow rate (m_N^*) and fluid flow resistance (R_N^*) at fixed heat transfer density.

ratio for minimum pressure drop and minimum pumping power. This method is also used for fixed heat transfer density without imposing any fluid flow condition.

4.2.1. Scale analysis of fluid flow optimization

The model and analysis developed in Sections 2 and 3 are now used for studying the optimal fluid flow conditions at a given (fixed) heat transfer density. Fig. 4 shows total mass flow rate $\dot{m}_N$ and fluid flow resistance R_N as function of x_*. Both variables are presented in its dimensionless form through $m_N^* = L^2 m_N'''/\mu$ with $m_N''' = N\dot{m}/(HWL)$ and $R_N^* = R_N(HWL)/\nu$ with $R_N = \Delta p/(N\dot{m})$, respectively. Increasing x_* imply decreasing mass flow rate together with increasing fluid flow resistance. Fig. 5 presents the parametric plot of dimensionless pressure drop and dimensionless pumping power with x_* shown along the curve. The two minima evidenced in this curve are $\Delta p_{\min}^* \Pr (Q_N^*/\varepsilon)^{-2} = 4.343$ and $(P_N^*/\varepsilon)_{\min} \Pr^2 (Q_N^*/\varepsilon)^{-3} = 6.033$, which correspond to $x_* \sim 0.043$ and $x_* \sim 0.102$, respectively. In view of the analysis of Section 2, and for thermally developing flow, these values of x_* do not depend on Pr, and thus are constant.

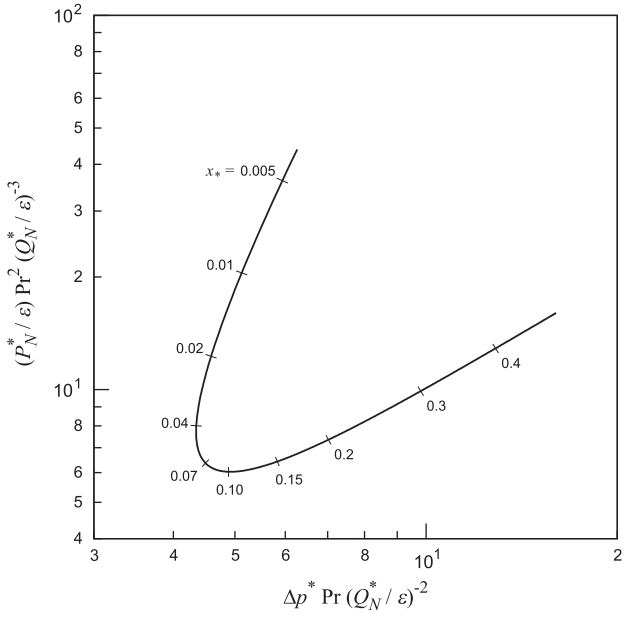

Fig. 5. Parametric plot of pressure drop and pumping power at fixed heat transfer density.

Also noticed in the Section 2 was the fact that maximization of Q_N^* with x_* as the free variable is equivalent to minimization of either Δp^* or P_N^*. Thus, the asymptotes derived in the previous section can be rearranged so as to predict the optimal heat sink designs corresponding either to minimum Δp^*, or to minimum P_N^*. In both cases the optimum dimensionless thermal length is the same, and is given by Eq. (41). On the other hand, from Eq. (45) we have

$$\Delta p_{\min}^* > 0.376 \left(2f\mathrm{Re}_{D_h}\right)^{1/2} \mathrm{Pr}^{-1} \left(Q_N^*/\varepsilon\right)^2, \tag{54}$$

where the sign > means that the actual minimum pressure drop is higher than the predicted value. Similarly, from Eq. (53) we have

$$(P_N^*/\varepsilon)_{\min} > 0.376 \left(2f\mathrm{Re}_{D_h}\right)^{1/2} \mathrm{Pr}^{-2} \left(Q_N^*/\varepsilon\right)^3. \tag{55}$$

Again, the sign > reminds that the actual pumping power is higher than the predicted value. We note that the factor $0.376(2f\mathrm{Re}_{D_h})^{1/2}$ is present in both the Eqs. (54) and (55). More remarkable is the result that the estimate of the optimum diameter is exactly the same either for $(\Delta p^*)_{\min}$ (Eqs. (11), (41), and (54)) or $(P_N^*)_{\min}$ (Eqs. (17), (41), and (55)) and is given by:

$$(D_h/L)_{\mathrm{opt}} \approx 1.630 \left(2f\mathrm{Re}_{D_h}\right)^{1/4} (Q_N^*/\varepsilon)^{-1/2}. \tag{56}$$

It is also interesting to note that the estimated $(D/L)_{\mathrm{opt}}$ ratio does not depend on Prandtl number, thus suggesting that firstly one may design geometrically the heat sink for the required heat transfer density, and then operate it in the optimal flow conditions according to the fluid in use. In the next section we proceed with a further examination of the implications of these results.

4.2.2. Intersection of asymptotes and fluid flow optimization

The results presented above justify a more close analysis of the relation between optimal design predicted by the method of the intersection of asymptotes and by fluid flow optimization. By inspection of Fig. 5 we note that the predicted optimum value $(x_*)_{\mathrm{opt}} \approx 0.067$ is located in between the values of x_* corresponding to the minima of Δp^* and P_N^*. Furthermore, it seems to be very close to the joint minimization of both these quantities. We explore this aspect by rewriting the asymptotes for a fixed heat transfer density without any fluid flow constraint and using two design variables: the D/L ratio that is related uniquely to the internal geometry; and the Reynolds number that is related to the fluid flow characteristics. In the following, for the sake of exemplification, thermally developing flow is considered with the values $Q_N^* = 5 \times 10^3$, $\varepsilon = 0.6$ and $\mathrm{Pr} = 5.0$.

The fully developed flow asymptote (small D and small Re) is derived as before by considering the outlet temperature approaching the wall temperature. Thus, by combining Eqs. (1), (2), and (29), with $U_0 = \nu \mathrm{Re}/D$ and Prandtl number $\mathrm{Pr} = \mu c_p/k$, we obtain the dimensionless heat transfer density in the form:

$$Q_{fd}^* = \varepsilon \mathrm{RePr} (L/D). \tag{57}$$

We conclude that in this limit the D/L ratio varies with Re at fixed Q_N^*.

The developing flow asymptote (large D and large Re) is derived using the boundary layer solution and assuming that the temperature of the fluid in the core flow approaches the inlet temperature. By combining Eqs. (33) and (39) with $x_* = (L/D)/(\mathrm{Re\,Pr})$, the dimensionless heat transfer density reads:

$$Q_{dv}^* = 4 \cdot 0.604 (f\mathrm{Re})^{1/3} \varepsilon (\mathrm{RePr})^{1/3} (L/D)^{5/3}. \tag{58}$$

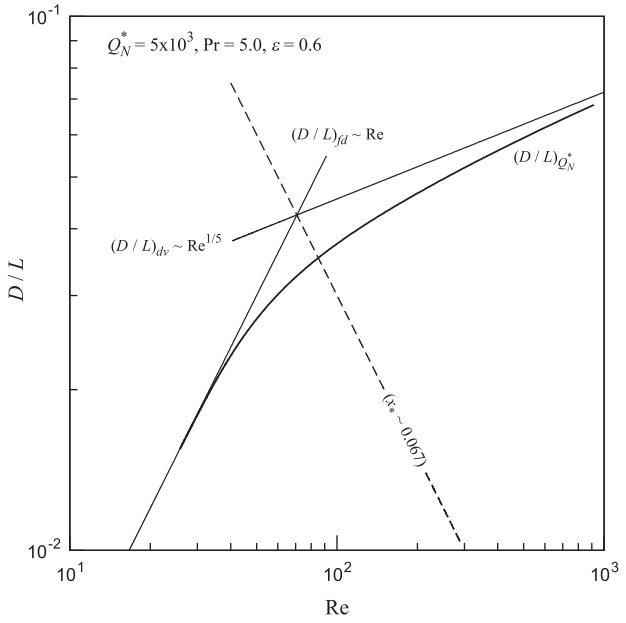

Fig. 6. Intersection of asymptotes at fixed heat transfer density and thermally developing flow.

Then, in this limit, for a fixed value of Q_N^* the D/L ratio varies with $\mathrm{Re}^{1/5}$.

The asymptotes of Eqs. (57) and (58) intersect each other at the dimensionless thermal length defined by Eq. (41) and at the D/L ratio given by Eq. (56), as expected, and as shown in Fig. 6 for the case of circular tubes analysed in the present work. In this case, however, it is particularly useful to find out the optimum D/L ratio along the Q_N^* curve (i.e., the point of intersection of the dashed line with the solid curve in Fig. 6). Thus, by using Eq. (6) with $U_0 = \nu\mathrm{Re}/D_h$ we obtain:

$$(D_h/L)_{\mathrm{opt}} = \left(\frac{1-\theta_{\mathrm{opt}}}{(x_*)_{\mathrm{opt}}}\right)^{1/2} (Q_N^*/\varepsilon)^{-1/2} \tag{59}$$

For thermally developing flow we have $(x_*)_{\mathrm{opt}} \approx 0.067$, $\mathrm{Nu}_{0-L} = 4.41$ and $\theta_{\mathrm{opt}} = 0.307$, and therefore the estimate of the optimum diameter given by Eq. (59) reduces to:

$$(D_h/L)_{\mathrm{opt}} = 3.221\,(Q_N^*/\varepsilon)^{-1/2}. \tag{60}$$

Again we verify that this estimate does not depend on Pr. Assuming that the numerical factor in the equation above is constant, in the same way as in the previous cases, to find out the optimum x_* as function of Pr for a simultaneously developing flow we can use the following expression:

$$\left(\frac{1-\theta_{\mathrm{opt}}}{(x_*)_{\mathrm{opt}}}\right)^{1/2} = 3.221. \tag{61}$$

The mean Nusselt number can be determined from correlations available in literature (e.g. [33]):

$$\mathrm{Nu}_{0-L} = \mathrm{Nu}_{fd}\left[1 + 0.067(x_*\mathrm{Pr})^{-0.62}\right]^{0.27}, \tag{62a}$$

$$\mathrm{Nu}_{fd} = \begin{cases} -0.5632 + 1.57x_*^{-0.3351}, & 10^{-6} \leqslant x_* \leqslant 10^{-3} \\ 0.9828 + 1.129x_*^{-0.3686}, & 10^{-3} \leqslant x_* \leqslant 10^{-2} \\ 3.6568 + 0.1272x_*^{-0.7373}\exp(-3.1563x_*), & x_* > 10^{-2} \end{cases} \tag{62b}$$

Because the mean Nusselt number varies inversely with Pr in the developing region, the optimum x_* decreases and tends to 0.067. The solution of Eq. (61) is presented and discussed in the next section. The values of pressure drop and pumping power that corresponds to these values of $(x_*)_{\mathrm{opt}}$ and $(D/L)_{\mathrm{opt}}$ along the curve Q_N^* (fixed) are now easily calculated using Eqs. (11) and (17), respectively.

We proceed by considering the graphical representation of D/L .vs. Re as some kind of map where not only the heat transfer density can be represented, the same happening with the other variables involved, thus allowing to find out the order of magnitude of the optimum diameter and Reynolds number that match the minima of Δp^* and P_N^*. Then from Eq. (11) with $x_* = (L/D)/(\mathrm{Re}\,\mathrm{Pr})$ one has;

$$(D/L)_{\Delta p} = \left(\frac{2f\mathrm{Re}}{\Delta p^*}\right)^{1/3} \mathrm{Re}^{1/3}. \tag{63}$$

Similarly, from Eq. (17):

$$(D/L)_{P_N} = \left(\frac{2f\mathrm{Re}}{P_N^*/\varepsilon}\right)^{1/4} \mathrm{Re}^{1/2}. \tag{64}$$

By considering $\Delta p^* = \Delta p^*_{\min}$ and $P_N^* = P^*_{N,\min}$ respectively in Eqs. (63) and (64), with $f\,\mathrm{Re} = 16$, the tangents to the Q_N^* curve can be drawn as shown in Fig. 7. Note that the points of tangency correspond to $x_* = 0.043$ and $x_* = 0.102$, respectively. The optimum values of D/L ratio and Reynolds number corresponding to the minima of Δp^* and P_N^* meet at the intersection of these lines, and the following function of $(x_*)_{\mathrm{opt}}$ is obtained

$$2\,(x_*)_{\mathrm{opt}} f\,\mathrm{RePr} = \frac{(\Delta p^*)^3_{\min}}{(P_N^*/\varepsilon)^2_{\min}}. \tag{65}$$

With the numerical values presented at the beginning of this section we have $x_* = 0.070$. This value is very close to that of the intersection of asymptotes. The solution of Eq. (65) for simultaneously developing flow is presented and discussed in the next section.

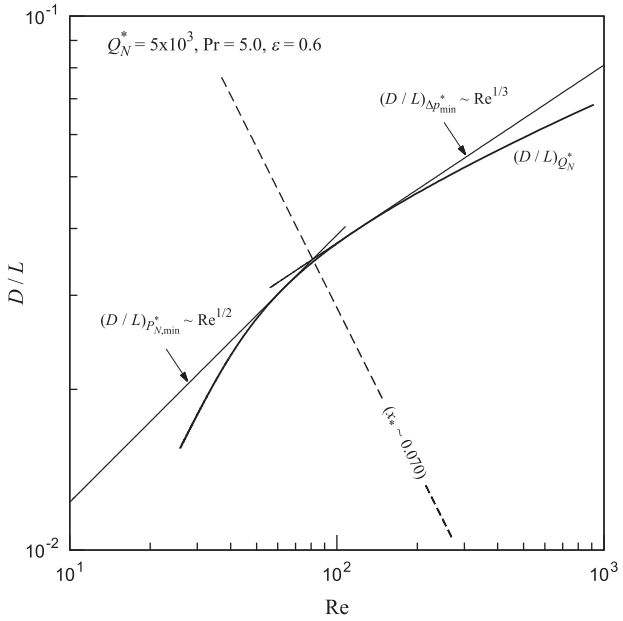

Fig. 7. Intersection of minimum Δp^* and minimum P_N^* limits at fixed heat transfer density and thermally developing flow.

5. Heat sink optimization results

In this section we present and discuss the main results of the present work according to the optimization objectives and the imposed constraints. The results are summarized in various tables in such a way that useful information is easily extracted, together with the equations for predicting the optimal heat sink design deduced in the previous section. The numerical results were obtained using the model described in Section 3.

5.1. Results of optimum dimensionless thermal length

When maximizing the heat transfer density and considering a thermally developing flow, the scale analysis carried out in the previous section shows that the optimum dimensionless thermal length $(x_*)_{opt}$ predicted by the method of the intersection of asymptotes is independent of the imposed fluid flow constraint (e.g. fixed pressure drop or fixed pumping power). The value $(x_*)_{opt} \approx 0.067$ was found to hold for circular tubes. In fact, it is possible to find out the fully developed and developing flow limits on which this method is based if diverse fluid flow conditions are imposed. In the case of simultaneously developing flow the values of $(x_*)_{opt}$ depends on the fluid flow constraint and Prandtl number due to the existence of a hydrodynamic boundary layer and to the relation between the hydrodynamic and thermal entrance lengths. These values of $(x_*)_{opt}$ are shown in Fig. 8 (dashed lines) as function of Prandtl number for a fixed value of Δp^* (from the solution of Eq. (44)) and for a fixed value of P_N^* (from Eq. (52)). For small Pr, the optimum dimensionless thermal length in the case of fixed Δp^* is slightly higher than in the case of fixed P_N^*, and in both cases $(x_*)_{opt}$ decreases with Pr , and tends to the value obtained for thermally developing flow. This is explained by the fact that the hydrodynamic entrance length is very small as compared with the thermal entrance length for higher Pr. The curve representing a fixed Q_N^* (from Eq. (61)) is not shown for concision, but some values are presented in Table 5. For increasing values of Pr we found a variation similar to that of the previous cases with values decreasing from $(x_*)_{opt} \approx 0.0722$ for Pr = 0.7 and tending to $(x_*)_{opt} \approx 0.067$. Also represented in the graph are the values of $(x_*)_{opt}$ obtained numerically through the model described in Section 3. The two series of values show the same dependency on Prandtl number as the estimated values, and tend to the values of x_* obtained for the case of thermally developing flow ($x_* \approx 0.043$ and $x_* \approx 0.102$, respectively). The values adapted from the work of Yilmaz et al. [20] for fixed Δp^* are presented for comparison. The results of Yilmaz's study were obtained using correlations for Nusselt number and are not expressed in terms of x_* thus requiring to be rewritten in terms of the solution of an equation similar to Eq. (44). In average, the estimated values of $(x_*)_{opt}$ surpass by 32% the numerical values in the case of fixed Δp^*, while in the case of fixed P_N^* the numerical values are underestimated by 48% in average. The differences between the predicted and the numerical results slightly increase with Prandtl number. The intersection of the fluid flow limits are calculated from Eqs. (8) and (65) and by using the values of minimum pressure drop and minimum pumping power obtained numerically. We can see that these values are very close to the values that emerge from the intersection of asymptotes and tend to $x_* \approx 0.070$.

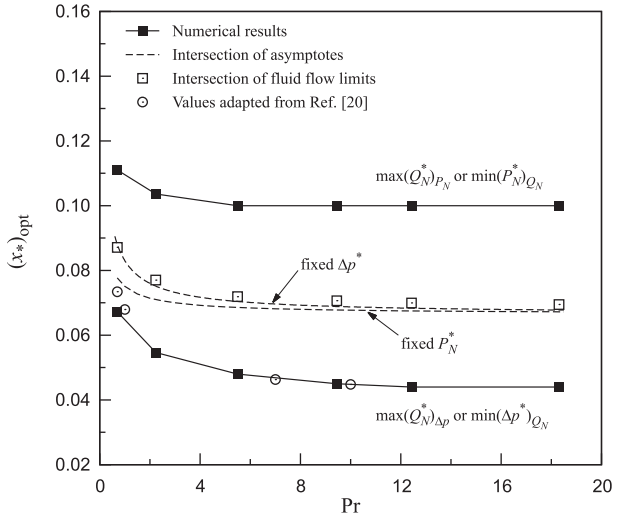

Fig. 8. Variation of $(x_*)_{opt}$ with the Prandtl number for minimum pressure drop, minimum pumping power, intersection of asymptotes and intersection of fluid flow limits.

5.2. Results of optimum diameter for the maximization of Q_N^*

The numerical results of $(D/L)_{opt}$ for maximum Q_N^* are summarized in Table 2. These values are in average 11% higher than the estimate of Eq. (43) for the case of fixed Δp^*, and for the values of Pr shown, while in the case of fixed P_N^* are in average 12% lower than the estimate of Eq. (51). The results of maximum heat transfer

Table 2
Optimum diameter of the tubes for maximum heat transfer density at fixed pressure drop $(D/L)_{opt}(\mathrm{Pr}\,\Delta p^*)^{1/4}$ and fixed pumping power $(D/L)_{opt}\mathrm{Pr}^{1/3}(P_N^*/\varepsilon)^{1/6}$ for different values of Pr number.

Pr	Fixed Δp^*	Fixed P_N^*
0.70	5.088	3.854
2.23	5.121	3.852
5.49	5.185	3.865
9.45	5.231	3.854
12.43	5.246	3.850
18.30	5.229	3.847
∞	5.223	3.814

Table 3
Maximum heat transfer density at fixed pressure drop $(Q_N^*/\varepsilon)_{max}(\mathrm{Pr}\Delta p^*)^{-1/2}$ and fixed pumping power $(Q_N^*/\varepsilon)_{max}\mathrm{Pr}^{-2/3}(P_N^*/\varepsilon)^{-1/3}$ and for different values of Pr number.

Pr	Fixed Δp^*	Fixed P_N^*
0.70	0.420	0.523
2.23	0.460	0.546
5.49	0.478	0.554
9.45	0.483	0.557
12.43	0.486	0.558
18.30	0.488	0.559
∞	0.480	0.549

Table 4
Optimum diameter of the tubes $(D/L)_{opt}(Q_N^*/\varepsilon)^{1/2}$ for minimum pressure drop and minimum pumping power at fixed heat transfer density.

Pr	Numerical	
	Minimum Δp^*	Minimum P_N^*
0.70	3.299	2.787
2.23	3.475	2.845
5.49	3.584	2.877
9.45	3.637	2.876
12.43	3.656	2.876
18.30	3.652	2.876
∞	3.619	2.826

Table 5
Numerical and predicted values of minimum $\Delta p^* \mathrm{Pr}\,(Q_N^*/\varepsilon)^{-2}$ and minimum $(P_N^*/\varepsilon)\mathrm{Pr}^2\,(Q_N^*/\varepsilon)^{-3}$ at fixed heat transfer density.

Pr	Numerical		Intersection of asymptotes		
	$(\Delta p^*)_{\min}$	$(P_N^*)_{\min}$	x_*	Δp^*	P_N^*
0.70	5.657	7.000	0.0722	5.698	7.606
2.23	4.718	6.152	0.0698	4.854	6.708
5.49	4.381	5.882	0.0685	4.602	6.479
9.45	4.281	5.795	0.0681	4.522	6.403
12.43	4.241	5.763	0.0678	4.505	6.406
18.30	4.203	5.730	0.0676	4.478	6.383
∞	4.343	6.033	0.0666	4.464	6.460

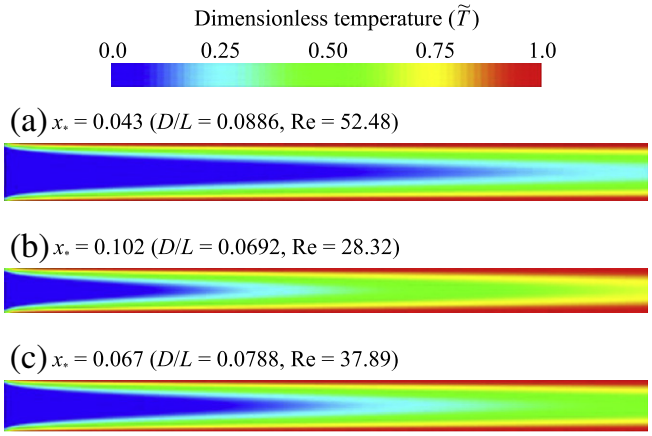

Fig. 9. Temperature field in an elemental tube for three distinct optimal designs: (a) minimum pressure drop; (b) minimum pumping power and (c) intersection of asymptotes ($Q_N^* = 1 \times 10^3$, Pr = 5.0, $\varepsilon = 0.6$).

density are summarized in Table 3, and show a mean difference of 13% as compared to the order-of-magnitude of Eq. (45) in the case of fixed Δp^* and of 17% compared with the estimate of Eq. (53) in the case of fixed P_N^*. These differences increase with Prandtl number in the case of $(D/L)_{\mathrm{opt}}$ while they decrease in the case of (Q_N^*/ε).

5.3. Results of optimum diameter for the fluid flow optimization

In Table 4 the values of the optimum diameter are presented for minimum pressure drop and minimum pumping power at fixed heat transfer density. These values are in average only 8% lower than the estimate of Eq. (56) in the first case, and 26% in the second. If compared with the more reasonable estimate of Eq. (60) we found mean differences of order 11% in both cases. A more noticeable result is presented in Table 5 that shows that the minimum pressure drop and the minimum pumping power are in average, respectively, 4% and 9% lower than the values obtained using the optimum diameter estimate of Eq. (60) together with Eq. (11) and Eq. (17).

Fig. 9 shows an example of the temperature field of a thermally developing flow within a single tube for three different heat sink designs with $Q_N^* = 1 \times 10^3$, $\varepsilon = 0.6$ and Pr = 5.0. The first temperature field corresponds to minimum pressure drop where the thermal boundary layer merge just at the tube outlet, while the second corresponds to minimum pumping power where the boundary layer merge approximately at the middle length of tube, and the third corresponds to the optimal design as defined from the intersection of asymptotes, the case in which the boundary layer merge closely before the tube outlet.

6. Conclusions

In the present work, we developed a set of theoretical results based on the method of intersection of asymptotes for predicting the optimal design of a heat sink composed of parallel tubes in a fixed volume and for various optimization objectives and imposed constraints. The estimated values were validated and complemented by numerical simulations. The optimization procedures lead to the following conclusions:

(a) *Maximization of heat transfer density with fixed pressure drop and fixed pumping power*. The estimate of the optimum dimensionless thermal length obtained through the method of the intersection of asymptotes is nearly independent of the constraints imposed to fluid flow and tends to a fixed value with increasing Pr. For lower values of Pr the predicted values of $(x_*)_{\mathrm{opt}}$ are slightly higher in the case of fixed pressure drop as compared to the values found for fixed pumping power. Estimates of optimum diameter of the tubes, and of the order of magnitude of maximum heat transfer density were obtained in both the case of fixed pressure drop and fixed pumping power. Results of the numerical procedure used for validation are also presented.

(b) *Minimization of pressure drop and pumping power with fixed heat transfer density*. The estimates of the optimum diameter provided the same value when considering either pressure drop minimization or pumping power minimization. The order of magnitude of minimum pressure drop and minimum pumping power are presented together with numerical results for comparison and validation. Additionally, it was found that the estimate of the optimum diameter does not depend on Prandtl number.

(c) *Joint minimization of Δp^* and P_N^* with fixed heat transfer density*. Scale analysis together with the method of the intersection of asymptotes was used in the case when heat transfer density is fixed. In this case two optimization variables are used: one of geometric nature that is represented by diameter to length ratio; and the other relative to fluid flow conditions, which is represented by the Reynolds number. The predicted $(x_*)_{\mathrm{opt}}$ is very close to the values corresponding to the case of joint minimization of pressure drop and pumping power. A more reasonable estimate of the optimum diameter is also presented together with the corresponding values of pressure drop and pumping power, which are found to overestimate the respective minima by only 4% and 9% in average.

Acknowledgements

The authors acknowledges the support of the Portuguese National Science Foundation – FCT (Fundação para a Ciência e Tecnologia) – through the Grant No. SFRH/BD/36840/2007, and the contract PTDC/EME-MFE/71960/2006.

References

[1] A. Bejan, Convection Heat Transfer, Wiley, New York, 1984, Problem 11, p. 157; Solutions Manual pp. 93–95.
[2] A. Bejan, E. Sciubba, The optimal spacing of parallel plates cooled by forced convection, Int. J. Heat Mass Transfer 35 (1992) 3259–3264.
[3] A. Bejan, Shape and Structure, from Engineering to Nature, Cambridge University Press, Cambridge, UK, 2000.
[4] J. Lewins, Bejan's constructal theory of equal potential distribution, Int. J. Heat Mass Transfer 46 (2003) 1541–1543.
[5] A.H. Reis, Constructal theory: from engineering to physics, and how flow systems develop shape and structure, Appl. Mech. Rev. 59 (2006) 269–282.

[6] A.H. Reis, A.F. Miguel, A. Bejan, Constructal theory of particle agglomeration and design of air-cleaning devices, J. Phys. D: Appl. Phys. 39 (2006) 2311–2318.
[7] A. Bejan, I. Dincer, S. Lorente, A.F. Miguel, A.H. Reis, Porous and Complex Flow Structures in Modern Technologies, Springer, New York, 2004.
[8] A. Bejan, A.H. Reis, Thermodynamic optimization of global circulation and climate, Int. J. Energy Res. 29 (2005) 303–316.
[9] A.H. Reis, C. Gama, Sand size versus beachface slope – an explanation based on the constructal law, Geomorphology 114 (2010) 276–283.
[10] A.H. Reis, A.F. Miguel, M. Aydin, Constructal theory of flow architecture of the lungs, Medical Phys. 31 (2004) 1135–1140.
[11] Y. Muzychka, Constructal design of forced convection cooled microchannel heat sinks and heat exchangers, Int. J. Heat Mass Transfer 48 (2005) 3119–3127.
[12] S. Mereu, E. Sciubba, A. Bejan, The optimal cooling of a stack of heat generating boards with fixed pressure drop, flowrate or pumping power, Int. J. Heat Mass Transfer 36 (1993) 3677–3686.
[13] A.J. Fowler, G.A. Ledezma, A. Bejan, Optimal geometric arrangement of staggered plates in forced convection, Int. J. Heat Mass Transfer 40 (1997) 1795–1805.
[14] A. Bejan, Optimal spacings for cylinders in crossflow forced convection, J. Heat Transfer 117 (1995) 767–770.
[15] G. Stanescu, A.J. Fowler, A. Bejan, The optimal spacing of cylinders in free-stream cross-flow forced convection, Int. J. Heat Mass Transfer 39 (1996) 311–317.
[16] T. Bello-Ochende, L. Liebenberg, J.P. Meyer, Constructal cooling channels for micro-channel heat sinks, Int. J. Heat Mass Transfer 50 (2007) 4141–4150.
[17] T. Bello-Ochende, J.P. Meyer, A. Bejan, Constructal ducts with wrinkled entrances, Int. J. Heat Mass Transfer 52 (2009) 3628–3633.
[18] T. Wen, F. Xu, T.J. Lu, Structural optimization of two-dimensional cellular metals cooled by forced convection, Int. J. Heat Mass Transfer 50 (2007) 2590–2604.
[19] Y.S. Muzychka, Constructal multi-scale design of compact micro-tube heat sinks and heat exchangers, Int. J. Thermal Sci. 46 (2007) 245–252.
[20] A. Yilmaz, O. Buyukalaca, T. Yilmaz, Optimum shape and dimensions of ducts for convective heat transfer in laminar flow at constant wall temperature, Int. J. Heat Mass Transfer 43 (2000) 767–775.
[21] P. Canhoto, A.H. Reis, Optimization of forced convection heat sinks with pumping power requirements, Int. J. Heat Mass Transfer 54 (2011) 1441–1447.
[22] W.M. Kays, M.E. Crowford, Convective Heat and Mass Transfer, McGraw-Hill, New York, 1993. pp. 108–158.
[23] Y. Muzychka, Analytical and Experimental Study of Fluid Friction and Heat Transfer in Low Reynolds Number Flow Heat Exchangers, Ph.D Thesis, Department of Mechanical Engineering, University of Waterloo, Ontario, Canada, 1999.
[24] Y.S. Muzychka, M.M. Yovanovich, Pressure drop in laminar developing flow in noncircular ducts: a scaling and modelling approach, J. Fluids Eng. 131 (2009) 111105. 11 p..
[25] Y.S. Muzychka, M.M. Yovanovich, Laminar forced convection heat transfer in the combined entry region of non-circular ducts, J. Heat Transfer Trans. ASME 126 (2004) 54–61.
[26] www.openfoam.com.
[27] M.A. Ebadian, Z.F. Dong, Forced convection, internal flow in ducts, in: W.M. Rohsenow, J.P. Harnett, Y.I. Cho (Eds.), Handbook of Heat Transfer, third ed., McGraw-Hill, New York, 1998.
[28] A. Bejan, Convection Heat Transfer, Wiley, New York, 1995.
[29] R.B. Bird, W.E. Stewart, E.N. Lightfoot, Transport Phenomena, Wiley, New York, 1960.
[30] S.W. Churchill, R. Usagi, A general expression for the correlation of rates of transfer and other phenomena, American Institute of Chemical Engineers 18 (1972) 1121–1128.
[31] R.K. Shah, A.L. London, Advances in Heat Transfer Supplement 1, Laminar Forced Flow Convection in Ducts, Academic Press, New York, 1978.
[32] S. Petrescu, Comments on the optimal spacing of parallel plates cooled by forced convection, Int. J. Heat Mass Transfer 37 (1994) 1283.
[33] B. Shome, Mixed convection laminar flow and heat transfer of liquids in isothermal horizontal circular tubes, Int. J. Heat Mass Transfer 38 (1995) 1945–1956.